

AB

PRECISION MEASUREMENT OF CHARGE SYMMETRY BREAKING IN np ELASTIC SCATTERING AT 347 MeV

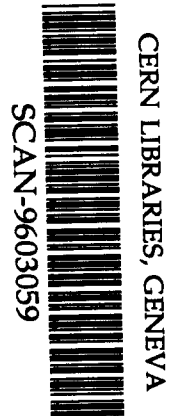
R. ABEGG¹, A.R. BERDOZ², J. BIRCHALL², J.R. CAMPBELL², C.A. DAVIS^{1,2},
P.P.J. DELHEIJ¹, L. GAN², P.W. GREEN^{1,3}, L.G. GREENIAUS^{1,3}, D.C. HEALEY¹,
R. HELMER¹, N. KOLB³, E. KORKMAZ³, L. LEE², C.D.P. LEVY¹, J. LI³, C.A. MILLER¹,
A.K. OPPER³, S.A. PAGE², H. POSTMA⁴, W.D. RAMSAY², J. SOUKUP³, G.M. STINSON³,
W.T.H. van OERS², A.N. ZELENSKI¹ and J. ZHAO²

¹ TRIUMF, 4004 Wesbrook Mall, Vancouver, B.C. V6T 2A3, Canada.

² University of Manitoba, Department of Physics, Winnipeg, Manitoba, R3T 2N2 Canada.

³ University of Alberta, Department of Physics, Edmonton, Alberta, T6G 2N5 Canada.

⁴ Technical University Delft, Laboratory for Technical Physics, 2600 GA, Delft, the Netherlands.



ABSTRACT

Charge symmetry breaking in np elastic scattering at 347 MeV has been measured with high precision. From fits of the measured asymmetry curves over the angular range $53.4^\circ \leq \theta_{cm} \leq 86.9^\circ$, the difference in the center-of-mass zero-crossing angles of the analyzing powers was determined to be $0.438^\circ \pm 0.054^\circ(\text{stat.}) \pm 0.051^\circ(\text{syst.})$. Using the experimentally determined slope of the analyzing power, $dA/d\theta = (-1.35 \pm 0.05) \times 10^{-2} \text{ deg}^{-1}$, this is equivalent to $\Delta A = [59 \pm 7(\text{stat.}) \pm 7(\text{syst.}) \pm 2(\text{syst.})] \times 10^{-4}$. Predictions of nucleon-nucleon interaction models based on meson exchange agree well with this result.

SW 9611

Isospin symmetry or charge independence in the NN system refers to the invariance of the NN interaction under arbitrary rotations in isospin space (isospace). Charge symmetry, which is a less restrictive symmetry, refers to the invariance of the interaction under a 180° rotation about the "2" axis in isospace. On the fundamental quark level, charge symmetry breaking (CSB) arises from the difference in the up and down quark masses and from the electromagnetic interaction among the quarks. The charge symmetry operator relates the up and down quarks as $P_{cs}|u\rangle = -|d\rangle$ and $P_{cs}|d\rangle = |u\rangle$ ^{1,2}. A detailed study of CSB, which shows at what level and how this symmetry is broken, will provide stringent constraints on NN potential models based on meson exchange theory and give insight into the applicability of such models at short distances. This will help to form a bridge between the meson-exchange based phenomenological NN potential models and the theory of quantum chromodynamics.

Isospin symmetry and charge symmetry breaking were first observed in the difference of the low energy NN scattering parameters^{2,3} and in the binding energy differences of mirror nuclei. The latter is the well-known Okamoto-Nolen-Schiffer effect^{4,5}. The non-zero difference of the 1S_0 scattering lengths, $\frac{1}{2}(a_{nn}^N + a_{pp}^N) - a_{np}^N = 5.7 \pm 0.3$ fm, shows charge independence breaking and the much smaller difference, $a_{nn}^N - a_{pp}^N = -1.5 \pm 0.5$ fm, shows charge symmetry breaking, with the superscript "N" denoting

*Written version of an invited talk given by W.T.H. van Oers.

the nuclear interaction part with the purely electromagnetic contribution removed². The Okamoto-Nolen-Schiffer effect is clearly seen in the 71 keV difference of the binding energies of 3H and 3He after subtraction of electromagnetic effects². However, conclusions from the latter two comparisons are clouded by non-negligible theoretical uncertainties, mainly in the corrections for the Coulomb interaction.

Studies of charge symmetry breaking in np elastic scattering have a unique advantage due to the absence of the Coulomb interaction. Charge symmetry in np elastic scattering leads to the separation of the isospin-singlet and isospin-triplet states. This in turn, leads to the decoupling of the spin-singlet and spin-triplet states and the equality of the analyzing powers⁶ when polarized neutrons are scattered from unpolarized protons and vice versa. Any non-zero difference of the analyzing powers, $\Delta A \equiv A_n - A_p$, where the subscripts denote the polarized nucleon, is clearly evidence for CSB. In np elastic scattering CSB is a manifestation of class IV forces in the classification scheme of Henley and Miller⁷ which mix the isospin-singlet and isospin-triplet states. Earlier measurements of CSB in np elastic scattering include the first such experiment ever at 477 MeV⁸ which yielded a result of $\Delta A = (47 \pm 22 \pm 8) \times 10^{-4}$, and a later, more precise experiment at 183 MeV⁹ which yielded a result of $\Delta A = (34.8 \pm 6.2 \pm 4.1) \times 10^{-4}$, where in both cases the first error is the statistical error and the second the systematic error and the results are at the zero-crossing angle of the average analyzing power. Theoretical calculations of CSB in np elastic scattering have been carried out with meson-exchange based NN potential models¹⁰⁻¹⁴. In these calculations the major contributions to ΔA stem from (1) the interaction of the proton current with the neutron magnetic moment (one photon exchange), (2) the np mass difference affecting charged pion exchange, and (3) the short range $\rho^0 - \omega$ mixing. Other smaller contributions include the np mass difference affecting ρ exchange and two-pion exchange, and other indirect quark effects. A contribution corresponding to $\pi - \gamma$ exchange has been evaluated recently and is found to be small¹⁵. While these theoretical calculations agree with earlier experiments, concerns¹⁶ have been raised regarding the application of on-shell meson mixing amplitudes to off-shell virtual processes such as $\rho^0 - \omega$ mixing. Various calculations¹⁷ have shown that off-shell effects have a significant influence on the contribution of $\rho^0 - \omega$ mixing to the observed difference of the analyzing powers. On the other hand, it has been pointed out^{2,14,18} that all available experimental results support theoretical calculations employing on-shell meson mixing amplitudes.

The experiment was performed with a 347 MeV neutron beam scattering off a frozen-spin proton target (FST). The neutron beam and the proton target were alternately polarized for the measurements of A_n and A_p , respectively. Identical beam and target properties (except polarization) and the same detection system were used for the interleaved measurements. Scattered neutrons and recoil protons were detected

in coincidence (within the c.m. angular range $\sim 50^\circ - 90^\circ$) by a mirror-symmetric detection system. This detection geometry results in the cancellation of geometric systematic errors to first order. Frequent flipping of the neutron beam or proton target spin directions cancelled systematic errors not correlated with spin directions. At the zero-crossing angle where the analyzing powers vanish, all systematic errors, except those correlated with spin direction reversals or due to background, were eliminated to at least second order. The details of a similar beam line, FST and detection system have been published earlier¹⁹⁻²⁰.

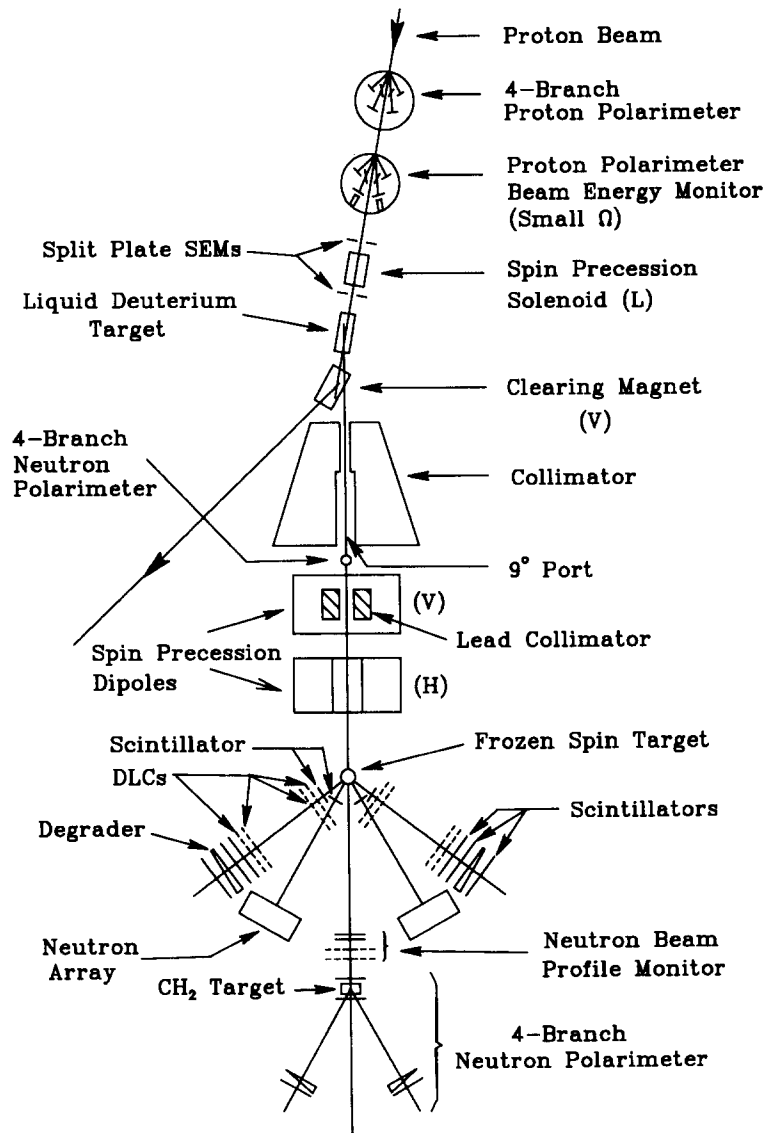


Figure 1: Layout of the beam transport system and schematic view of the experimental apparatus.

A 369 MeV polarized proton beam was obtained from the TRIUMF cyclotron with an optically-pumped polarized ion source. Proton beam polarization and energy were monitored by two polarimeters and a beam energy monitor, respectively. Figure 1 displays a schematic of the beam line layout and the experimental apparatus. The 347 MeV neutron beam (polarized or with zero transverse polarization depending on the phase of the experiment) was produced via the $D(p,n)2p$ reaction using an incident proton beam with a typical intensity of $1.8 \mu\text{A}$ and an average polarization (for the polarized neutron beam phase of the experiment) of $(71.7 \pm 1.4)\%$ incident on a 0.214 m long LD_2 target. The proton beam position on the LD_2 target was stabilized (to ± 0.05 mm) using a set of split-plate secondary electron emission monitors, coupled via a feedback system to two sets of steering magnets. The proton polarization was rotated from an initial vertical (transverse) direction to the sideways (horizontal) direction by a superconducting solenoid. The large value of the sideways to sideways polarization transfer coefficient, $r_t \simeq -0.88$ at 363 MeV, in the neutron production reaction yielded an average neutron polarization of $(61.2 \pm 1.8)\%$. The neutron beam was defined by a tapered 3.3 m long steel collimator which gave a neutron beam profile encompassing the FST cell. The initial sideways component of the neutron polarization was precessed into the vertical direction by a combination of two dipole magnets. The neutron beam profile and polarization were monitored continuously by a neutron profile monitor and two neutron polarimeters, respectively.

The FST contained a $20 \times 50 \times 35 \text{ mm}^3$ (width \times height \times length) sample cell filled with 2 mm diameter butanol beads immersed in the $^3\text{He}/^4\text{He}$ mixture of the dilution refrigerator. It was located 12.85 m downstream of the LD_2 target, and achieved an average polarization of $(73.2 \pm 2.2)\%$. During data recording the proton polarization was maintained by a 0.22 T holding field. The recoil protons were detected by time-of-flight (TOF)/range telescopes covering the angular range 42.5° - 63.5° (lab). Each proton telescope consisted of a TOF start scintillator, four delay line wire chambers, two scintillator E-counters, a brass wedge-shaped degrader and a veto scintillator counter, all aligned along the nominal recoil proton direction of 53.00° . The scattered neutrons were detected by scintillation detector arrays placed so as to span $24.0^\circ - 42.4^\circ$ (lab). Each neutron detector consisted of a main neutron detector array and an auxiliary detector array. Each main neutron detector array was made of two banks of seven scintillator bars placed horizontally, one bank behind the other. Each auxiliary array was made of a single bank of two scintillator bars placed vertically. Each scintillator bar had dimensions of $0.15 \times 0.15 \times 1.05 \text{ m}^3$.

Throughout the data taking periods, the various system parameters, such as the proton beam energy, the proton and neutron beam positions, the beam and target polarizations, and the precession magnets and holding field settings were kept within specified strict limits in order to maintain stringent control of possible sources of

systematic errors. A full cycle of data taking, which took four days to complete, consisted of different beam and FST polarization states, different FST holding field directions, and reversal of the last spin precession magnet polarity. This optimized the cancellation of systematic errors. To study background, data were taken with carbon beads of an equivalent target thickness replacing the butanol beads in the FST, with the rest of the target and its operational conditions unchanged.

Data analysis proceeded through the following phases: a) assessment of the sources of systematic error; b) extraction of the elastic np scattering events, the asymmetry angular distributions, and the zero-crossing angles of the asymmetry angular distributions; c) corrections for the contributions due to quasi-elastic (n,np) background and for the difference in the *effective* average neutron beam energy for the polarized and unpolarized phases arising from the neutron energy-polarization correlation.

To identify free np elastic scattering events cleanly, recoil proton and scattered neutron tracks were reconstructed. Their kinetic energies were calculated from the respective TOFs from the target to the E-counters or neutron detector arrays. Distributions giving unambiguous signatures of two-body kinematics were constructed. The kinematical variables tested consisted of opening angle, coplanarity angle, horizontal momentum balance, and the kinetic energy sum of the coincident neutron-proton pairs. Momentum dependent χ^2 distributions were calculated to account for broadening of the kinematical variables due to multiple scattering. Various cuts were applied to either the individual χ^2 distributions or to a summed χ^2 . Approximately 25% of the total events passed the cuts applied.

The holding field of the FST caused either a clockwise or a counterclockwise deflection of the recoil protons ranging from 1.0° to 1.8° . From the regions where the left and right detection arms covered the same range of angles (comprising 91% of the np elastic scattering events), the scattering asymmetries were extracted as a function of proton scattering angle (θ_p) using the formula $\epsilon = \frac{r-1}{r+1}$, where $r = \sqrt{\frac{L^+R^-}{L^-R^+}}$. The “+” and “-” superscripts denote the spin states, and the quantities “L” and “R” denote the counts for left and right scattered events in a particular angle bin. The zero-crossing angles, θ_o , were deduced from fits to the asymmetry angular distributions. To calculate ΔA from the measured $\Delta\theta_o$, $dA/d\theta$ is required. Because $dA/d\theta$ as given by various phase shift analyses exhibits large variations and the FST polarization is known to about 3% of its value, the experimentally determined $dA/d\theta$ was considered superior to estimates from phase shift analyses. CSB has a negligible effect on the value of $dA/d\theta$ compared to the experimental uncertainty in the FST polarization.

Monte Carlo simulations were made to study the neutron beam production reaction $D(\vec{p}, \vec{n})2p$. The simulated neutron beam profile and energy distributions were

compared to the experimental measurements; good agreement was achieved. The difference between the *effective* average neutron energy for the polarized and unpolarized beams (to account for the different weighting of the neutron beam spectra) was calculated, based on the simulated distributions, to be (-0.54 ± 0.11) MeV. The energy dependence of the zero-crossing angle, $d\theta_o/dE = (-0.0475^\circ \pm 0.0025^\circ)/\text{MeV}$, as deduced from phase shift analyses²¹ was applied to determine a correction of $+0.026^\circ \pm 0.005^\circ$ (c.m.) in the zero-crossing angle of A_n . Background data obtained with the target filled with carbon beads were analyzed in an identical fashion to the butanol target data. It was determined that about 4% of the events which passed the cuts were from the background and that the analyzing power of the background is $A_b = -0.004 \pm 0.007$ at the zero-crossing angle. Based on these evaluations, a correction of $\Delta A = (-1.6 \pm 2.8) \times 10^{-4}$ for the background contribution was applied to the result.

The extracted value of the zero-crossing angle difference is $\Delta\theta_o = 0.438^\circ \pm 0.054^\circ(\text{stat.}) \pm 0.051^\circ(\text{syst.})$ (c.m.) deduced from fits of the asymmetry distributions over the angle range $53.4^\circ \leq \theta_{cm} \leq 86.9^\circ$. (See Figure 2 for a typical asymmetry angular distribution). Although the individual zero-crossing angles show a dependence on the functional form chosen for the fit of the asymmetry angular distribution, the zero-crossing angle difference is rather insensitive to the functional form. An estimate of the corresponding systematic error was derived using different functional forms and is included in the final result. Employing $dA/d\theta_{cm} = (-1.35 \pm 0.05) \times 10^{-2} \text{ deg}^{-1}$, determined from the measured asymmetries with the FST polarized, the value of ΔA at the zero-crossing angle is $[59 \pm 7(\text{stat.}) \pm 7(\text{syst.}) \pm 2(\text{syst.})] \times 10^{-4}$. The second systematic error quoted for ΔA arises from the uncertainty in the experimentally determined slope of the analyzing power.

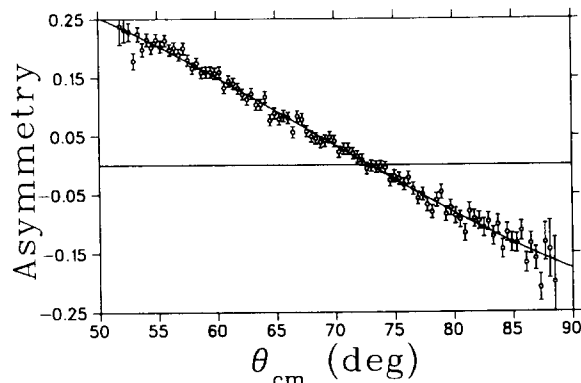


Figure 2: A sample asymmetry angular distribution obtained with the FST polarized, the FST holding field direction pointing vertically up and the last spin precession dipole magnet field direction pointing to the left. The angular distribution was fitted by a third degree polynomial in $(\theta - \theta_o)$ in order to determine $\hat{\theta}_o$.

The non-zero difference, $\Delta A \equiv A_n - A_p$, measured in the present experiment represents the strongest and least ambiguous evidence for CSB in the nuclear interaction. When the electromagnetic contribution of one photon exchange is removed, leaving only the strong NN interaction, the difference in the analyzing powers, $\Delta A \equiv A_n - A_p$, is five standard deviations away from zero. The theoretical predictions of Holzenkamp, Holinde and Thomas¹² (HHT) and Iqbal and Niskanen¹⁴ (IN), agree well with the result of this experiment. Figure 3 shows a comparison of the predictions of HHT and IN with the three existing measurements of ΔA . Existing theories concur with all three measurements underscoring the success of modern meson exchange theories at describing nucleon-nucleon scattering.

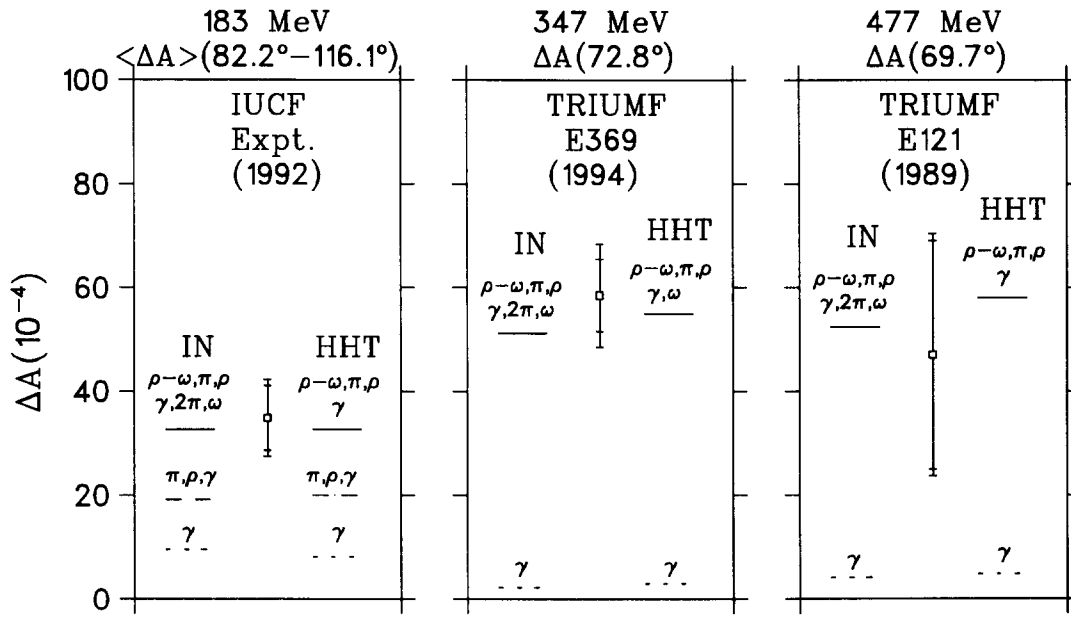


Figure 3: A summary of the existing measurements of CSB in np elastic scattering and comparison of the theoretical calculations by Iqbal and Niskanen, Ref. 14 (IN) and Holzenkamp, Holinde and Thomas Ref. 12 (HHT). The inner error bars on the data points represent the statistical errors and the outer error bars represent the quadrature sum of the systematic and statistical errors. The horizontal lines are the various summed contributions obtained from IN and HHT (γ : one photon exchange; π, ρ , and 2π : np mass difference affecting π, ρ and 2π exchanges; $\rho - \omega$: $\rho^0 - \omega$ mixing). Note that the $\rho^0 - \omega$ mixing contribution at the two higher energies is small since it changes sign close to the zero-crossing angle of the average analyzing power.

Work supported in part by the Natural Sciences and Engineering Research Council of Canada.

References

1. G.A. Miller, B.M.K. Nefkens and I. Slaus, *Phys. Rep.* **194**, 1 (1990).

2. G.A. Miller and W.T.H. van Oers, in *Symmetries and Fundamental Interactions in Nuclei*, ed. W.C. Haxton and E.M. Henley (*World Scientific Publishing Co., Singapore*), in press.
3. O. Dumbrajs et al., *Nucl. Phys. B* **216**, 277 (1983).
4. K. Okamoto, *Phys. Lett.* **11**, 150 (1964).
5. J.A. Nolen, Jr. and J.P. Schiffer, *Ann. Rev. Nucl. Sci.* **19**, 471 (1969).
6. P. LaFrance and P. Winternitz, *J. Physique* **41**, 1391 (1980).
7. E.M. Henley and G.A. Miller, in *Mesons in Nuclei*, ed. M. Rho and D.H. Wilkinson (North-Holland Publishing Co., Amsterdam, 1979) p. 407 .
8. R. Abegg et al., *Phys. Rev. D* **39**, 2464 (1989).
9. S.E. Vigdor et al., *Phys. Rev. C* **46**, 410 (1992); private communication (1994).
10. L. Ge and J.P. Svenne, *Phys. Rev. C* **33**, 417 (1986); *C* **34**, 756 (E) (1986).
11. A.G. Williams, A.W. Thomas and G.A. Miller, *Phys. Rev. C* **36**, 1956 (1987).
12. B.H. Holzenkamp, K. Holinde and A.W. Thomas, *Phys. Lett. B* **195**, 121 (1987).
13. M. Beyer and A.G. Williams, *Phys. Rev. C* **38**, 779 (1988).
14. M.J. Iqbal and J.A. Niskanen, *Phys. Rev. C* **38**, 2259 (1988); private communication (1994).
15. J.L. Friar and S.A. Coon, private communication (1995).
16. T. Goldman, J.A. Henderson and A.W. Thomas, *Few Body Problems* **12**, 123 (1990).
17. G. Krein, A.W. Thomas and A.G. Williams, *Phys. Lett. B* **317**, 293 (1993); J. Piekarewicz and A.G. Williams, *Phys. Rev. C* **47**, R2462 (1993); T. Hatsuda et al., *Phys. Rev. C* **49**, 452 (1994); M.J. Iqbal and J.A. Niskanen, *Phys. Lett. B* **322**, 7 (1994); K. Saito and A.W. Thomas, *Phys. Lett. B* **335**, 17 (1994); K.L. Mitchell et al., *Phys. Lett. B* **335**, 282 (1994); H.B. O'Connell et al., *Phys. Lett. B* **336**, 1 (1994).
18. T.D. Cohen and G.A. Miller, *private communication* (1995).
19. R. Abegg et al., *Nucl. Instr. and Meth.* **A234**, 11 (1985); *ibid* **A234**, 20 (1985).
20. P.P.J. Delheij, D.C. Healey, and G.D. Wait, *Nucl. Instr. and Meth.* **A264**, 186 (1988);
21. R.A. Arndt, *Interactive dial-in program SAID*, solution SM94.